Volume 9, Issue 4, 2019, 4150 - 4156 **ISSN 2069-5837**

Biointerface Research in Applied Chemistry

www.BiointerfaceResearch.com

https://doi.org/10.33263/BRIAC94.150156

Original Research Article **Open Access Journal**

Received: 29.06.2019 / Revised: 07.08.2019 / Accepted: 10.08.2019 / Published on-line: 15.08.2019

Molecular structure, electronic properties, vibrational analysis and reactivity parameters Of (Z)-N-(4-methoxyphenyl)-2-(4-oxothiazolidin-2-ylidene)acetamide: a theoretical study

Prem Chandra Maurya [1], Krishna Kant Yadav [1], Amarendra Kumar [1,*]

[1]Department of Physics, University of Lucknow, India

*corresponding author e-mail address:***akgkp25@yahoo.co.in**

ABSTRACT

Thiazolidine having important medicinal properties have been under investigation for a long time. In a recent study, A. Galushchinskiy et. al. synthesized and studied the crystal structure of thiazolidine derivative (Z)-N-(4-Methoxyphenyl)-2-(4-oxothiazolidin-2-ylidene)acetamide (MPOA). Keeping biological activity of thiazolidine in mind, quantum chemical calculations of energies, geometrical structure and vibrational wave numbers were carried out by DFT methods with 6-311++G(d,p) basis sets. A study on the electronic, dipole moment and frontier molecular orbital energies were also performed. HOMO and LUMO energy gap confirm the occurring of charge transformation in the molecule. The Frontier Molecular Orbital's (FMO), Molecular Electrostatic Potential were studied. The theoretical IR for the title compound has been also calculated. Molecular electrostatic potential surfaces and various reactivity parameters have also been studied to explain the reactive nature of compound.

Keywords: *Molecular Structure, Frontier molecular orbitals, MEPS ,Vibrational Analysis, Reactivity Parameters.*

1. INTRODUCTION

Thiazolidines, a heterocyclic compound has been studied for a long time because of their importance in medicinal chemistry. It possess various biological activities such as antimicrobial [1], antibacterial, antifungal, antipsychotic, antiubercular, ani-cancer [2-4], anti HIV, cyclooxygenase inhibitory, anti-histaminic, anti- platelet activating factor Ca2+ channel blocker, antioxidant, anti-inflammatory, analgesic and diabetes mellitus types-2 activity [5-10]. Keeping above mentioned biological properties of thiazolidine, one of its derivative (Z)-N-(4-Methoxyphenyl)-2-(4-oxothiazolidin-2-ylidene)acetamide (MPOA) has been studied using theoretical quantum chemical method for its vibrational and electronic properties. Various local and global reactivity descriptors of the title compound have also been calculated and explained.

2. MATERIALS AND METHODS

In the present study,density functional theory calculations were performed using DFT with Becke-3-Lee-Yang-Parr (B3LYP) [11,12] combined with 6-311++G(d,p) basis sets using GAUSSIAN 09W program package. The calculated frequencies are scaled down with factor 0.9648 to yield the coherent with the observed frequencies [13]. The vibrational wavenumber assignment hasbeen done by combining the result of the Gauss view 5 program, symmetry considerations and VEDA 4 program. Molecular electrostatic potential surface (MESP) has been computed at the same level of theory and plotted using Gauss-view 5 program.

3. RESULTS

3.1.Molecular geometry.

In quantum chemical calculation the optimization of geometry is the primary task and playa key role. So we have been optimized molecular geometry of the title compound by energy minimization using DFT at the B3LYP level of theory and the split valence basis set 6-311++G (d,p). It confirms to be located at the local true minima on potential energy surface.The optimized molecular structure thus obtained with the numbering scheme of the atoms in fig 1.The comparative optimized structural parameters (bond lengths, bond angles and dihedral angles) are listed in Table 1. For the title compound, all C-C bond lengths in benzene ring lies in the range 1.387- 1.404 Å and in five membered ring carbon–carbon bond length is 1.519 Å, carbon–nitrogen bond length lies in the range 1.380Å- 1.416Å, C-S bond length lies between 1.770Å-1.843 Å.In addition to benzene ringand five membered ring C-C bonds, other carbon–carbon bond length C17-C18 is 1.463 Å, C18-C20 is 1.353 Å, also the bondlength between carbon and oxygen i.e. C12-O3 and C24-O9 are 1.367 Å and 1.209 Å. The C-H bond lengths in six member ringand methoxy group lies in the range 1.078-1.086 Å, and 1.088Å-1.095Å respectively, and it is found 1.907 Å in five member ring.

All the calculated bond lengths are in full agreement with experimental values reported by A. Galushchinskiy et.al [14].

The endocyclic bond angle in benzene ring lies in the range 118.7˚-121.4˚. In five member ring the bond angle C20–S1-C21, S1-C21-C24, N6-C24-C21, C20-N6-C24, O9-C24-N6 are found to be 91.6˚, 108.3˚, 109.8˚, 119.7˚, 124.3˚ respectively and bond angles N6-C20-C18, C20-C18-C17, C18-C17-N2, C17-N2-C4, N2-C4-

C7 and C17-C18-H19, C17-N2-H29, C4-N2-H29 are calculated at 123.3°, 121.0°, 114.4°, 129.3°, 117.7° and120.3°, 115.9°, 114.8° respectively, other angles O9-C24-C21, C18-C17-O5, N2-C17-O5, O3-C12-C10, C13-C12-O3, C25-O3-C12 are found to be 125.9°, 122.0°, 123.5°, 124.7°, 116.2°, 118.4° respectively. In five membered ring C24-N6-H30 is found to be 118.9° respectively, angles C20-C18-H19 ,C20-N6-H30, C24-C21-H22, C24-C21-H23, H22-C21-H23, S1-C21-H23, S1-C21-H22 are calculated at 118.7°, 121.4° 109.2°, 109.2°, 108.7°, 110.7°, 110.7° respectively. All the calculated valuesarenearly good matched with experimental values [14]. The dihedral angle in benzene ring is found between 0° or 180° and show agreement with the experimental values. In methoxy group angle C25-O3-C12-C13, C7-C10-C12-O3, O3-C12-C13-C15 are 180°, -180°, 180° respectively which shows that this group is in same plane as that of benzene ring. In five member ring the dihedral angle are found 0° or 180° which is in good agreement with experimental value and reveals that the five member ring is planer. The dihedral angle C17-N2-C4-C7, C4-N2-C17-O5, C4-N2-C17-C18 are calculated 180°, 0°, -180° respectively and nearly same to the experimental data [14].

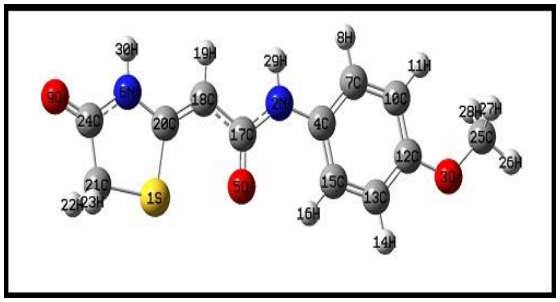

Figure 1. Optimized molecular geometry of MPOA at B3LYP/6-311++G (d,p).

Table 1. Geometrical parameters of optimized geometry of MPOA.

Parameter	Calculated values	Experimental values
Bond length(angstrom)		
S1- C20	1.77	1.74
S1-C21	1.84	1.80
N2-C4	1.41	1.40
N2-C17	1.37	1.35
N2-H29	1.00	0.96
O3-C12	1.36	1.37
03-C25	1.41	1.40
C4-C7	1.39	1.38
C4-C15	1.39	1.38
O5-C17	1.23	1.24
N6-C20	1.38	1.39
N6-C24	1.38	1.34
N6-H30	1.01	0.92
C7-H8	1.08	0.93
C7-C10	1.39	1.38
O9-C24	1.20	1.20
C10-H11	1.08	0.93
C10-C12	1.40	1.38
C12-C13	1.40	1.38
C13-H14	1.08	0.93
C13-C15	1.39	1.38
C15-H16	1.08	0.93
C17-C18	1.46	1.44
C18-H19	1.09	0.93
C18-C20	1.35	1.33
C21-H22	1.09	0.97
C21-H23	1.09	0.97
C21-C24	1.51	1.50
C25-H26	1.09	0.96
C25-H27	1.10	0.96
C25-H28	1.09	0.96
Bond angle (in degree)		
C20-S1-C21	91.6	92.1
C4-N2-C17	129.3	128.8
C4-N2-H29	114.8	112.1
C17-N2-H29	115.9	119.0
C12-O3-C25	118.4	117.4
N2-C4-C7	117.7	117.9
N2-C4-C15	123.7	122.8
C7-C4-C15	118.7	119.1
C20-N6-C24	119.7	118.4
C20-N6-H30	121.4	120.5
C24-N6-H30	118.9	121.0
C4-C7-H8	119.8	119.3
C4-C7-C10	121.4	121.4
H8-C7-C10	118.8	119.3
C7-C10-H11	119.0	120.3
C7-C10-C12	119.6	119.3
H11-C10-C12	121.4	120.3
O3-C12-C10	124.7	125.0
O3-C12-C13	116.2	115.7
C10-C12-C13	119.1	119.3
C12-C13-H14	118.5	119.2
C12-C13-C15	121.3	121.6
H14-C13-C15	120.2	119.2
C4-C15-C13	119.9	119.1
C4-C15-H16	119.5	120.4
C13-C15-H16	120.6	120.4
N2-C17-O5	123.5	123.1
N2-C17-O5	114.4	123.1
O5-C17-C18	122.0	122.0
C17-C18-H19	120.3	119.1
C17-C18-C20	121.0	121.7
H19-C18-C20	118.7	119.1
S1-C20-N6	110.6	110.6
S1-C20-C18	126.0	126.6
N6-C20-C18	123.3	122.8
S1-C21-H22	110.7	110.1
S1-C21-H23	110.7	110.1
S1-C21-C24	108.3	107.8
H22-C21-H23	108.7	108.5
H22-C21-C24	109.2	110.1
H23-C21-C24	109.2	110.1
N6-C24-O9	124.3	125.1
N6-C24-C21	109.8	111.1
O9-C24-C21	125.9	123.8
O3-C25-H26	105.9	109.5
O3-C25-H27	111.5	109.5
O3-C25-H28	111.5	109.5
H26-C25-H27	109.2	109.5
H26-C25-H28	109.3	109.5
H27-C25-H28)	109.4	109.5
Dihedral Angles(degree)		
C21-S1-C20-N6	-0.00	-1.8
C21-S1-C20-C18	180.0	179.6
C20-S1-C21-C24	0.0	1.19
C17-N2-C4-C7	180.0	-163.6
C17-N2-C4-C15)	-0.0	20.8
C4-N2-C17-O5	0.0	1.7
C4-N2-C17-C18	-180.0	-176.5
C25-O3-C12-C13	180.0	175.8
N2-C4-C7-C10	180.0	-177.8
N2-C4-C15-C13	-180.0	177.4
C7-C4-C15-C13	-0.0	1.9
C24-N6-C20-S1	0.0	2.2
C24-N6-C20-C18	-180.0	-179.2
C20-N6-C24-O9	180.0	179.9
C20-N6-C24-C21	-0.0	-1.2
C4-C7-C10-C12	0.0	-1.0
C7-C10-C12-O3	-180.0	-176.4
C7-C10-C12-C13	0.00	4.1
O3-C12-C13-C15	180.0	176.1
C10-C12-C13-C15	-0.0	-4.2
C12-C13-C15-C4	0.0	1.2
N2-C17-C18-C20	-180.0	176.9
O5-C17-C18-C20	-0.0	-1.5
C17-C18-C20-S1	-0.0	1.6
C17-C18-C20-N6	180.0	-176.9
S1-C21-C24-N6	0.0	-0.2
S1-C21-C24-O9	-180.0	178.6

3.2 Frontier molecular orbitals.

In the field of quantum chemistry research, the significant orbitals HOMO and LUMO are the orbitals involved in the reactivity of chemical compounds and also known as frontier molecular orbital (FMO). HOMO is the highest occupied molecular orbital (orbital with highest energy) so from this orbital the electrons can be easily removed by donating (nucleophilic) electron density to form a bond which act as Lewis base or facilitate oxidation. LUMO is the lowest unoccupied molecular orbital (orbital with lowest energy) which is empty so accepting (electrophilic) more electrons into this orbital act as Lewis acid or helps in reduction. The HOMO and LUMO arenot always involved in chemical reactivity but if HOMO-LUMO is not symmetrical then HMOM-1 and LUMO +1 involved in the reaction. The difference between HOMO energy eigenvalue and LUMO energy eigenvalue is known as HOMO- LUMO gap The negative value of HOMO and LUMO energy is calculated as the ionization potential(IP) and electron affinity(EA) respectively (Koopmans's approximation). The chemical reactions and resonance can be explained with the help of HOMO- LUMO on one or more molecules. The 3D structure of Frontier molecular orbital of the title compound shown in fig 2.

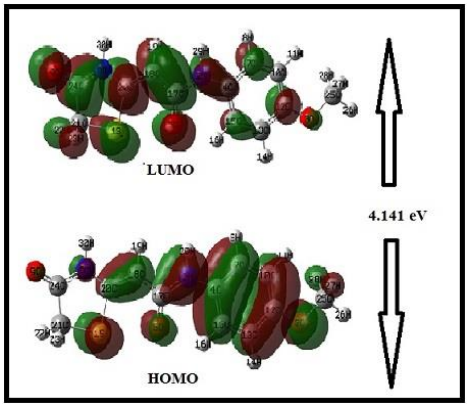

Figure 2.HOMO-LUMO Plot of MPOA.

The HOMO lies at -5.693 *eV* and LUMO lies at -1.552 *eV* respectively. HOMO is delocalized over the benzene ring and partially to five membered ring, while LUMO is delocalized over the five membered ring and partially to benzene ring and shows Rydberg characterwhich leads to the charge transfer within the molecule. The frontier molecular orbital energy gap is found to be 4.141eV. This energy gap being low predicts reactive nature of the compound under consideration.

3.3 Molecular electrostatic potential (MEPS).

The contributions of the molecular electronic charge and of the nuclei α give the molecular electric potential as

$$\Phi(x_1,y_1,z_1) = \sum_{\alpha}^{Z}\alpha\ e/4\pi\varepsilon_0 r_{12} - e\iiint \rho(x_2, y_2, z_2)\ /4\pi\varepsilon_0 r_{12}\ dx_2 dy_2\ dz_2$$

Where r_{12} is the distance between points 1and 2 and the integration is overall space. In atomic units the e and $4\pi\varepsilon_0$ disappear in this equation. Molecular electrostatic potential surface opens a door to predict the reactive sites for electrophilic (electron accepting, i.e. negative region) and nucleophilic (electron donating i.e. positive region) attack as well as hydrogen bonding interactions in a molecule. MEPS were calculated at the B3LYP/6-311++G(d,p) of optimized geometry of the molecule is depicted in fig 3. The importance of MESP lies in the fact that it simultaneously displays molecular size, shape as well as positive, negative and neutral electrostatic potential regions in terms of color grading.

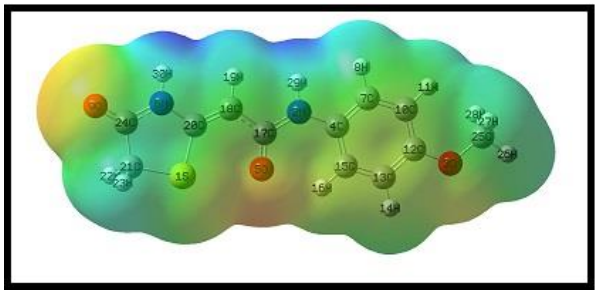

Figure 3. Molecular electrostatic potential Surfaces (MEPS) of MPOA.

The individual color indicates the different values of electrostatic potential. The red color at the surface represents negative regions (electrophilic reactivity) while blue color represents positive regions(nucleophilic reactivity) and green color shows the neutral potential regions for a molecule. The negative regions in the molecule are localized mainly on the electronegative atoms. A positive region is concentrated on the hydrogen group of the molecule acting as a possible site for nucleophilic attack. The addition of electron withdrawing groups increase the positive potential at the center of the ring. The variation in ESP surfaces shows an increase in the intensity of this localized positive potential in the molecule and it becomes more electron-deficient. Thus the ESP surface measurements identify two complementary regions within the compound. Electrophiles (electron-deficient, positively charged species) tend to be attracted to the regions of a molecule in which the ESP attains its most negative values since these are the effects of molecule's electrons are most dominant, whereas nucleophiles (an electron rich, negatively charged species) are especially attracted to the areas where the ESP is the most positive.

3.4 Vibrational analysis and IR spectrum.

The vibrational frequency assignments are carried out by combining the result of the VEDA 4 program and Gauss View 5.0 program with symmetry considerations. Vibrational frequency are calculated at B3LYP/6311++(d,p) level of theory because at this level theory vibrational wavenumbers are known to be higher than the experimental values due to non-inclusion of anharmonicity effect, so that calculated frequencies are scaled with the factor of 0.9648 in order to compensate for anharmonicity of vibrations as devised by Merrick et al. [8].Theoretical IR spectra are plotted in fig.3. The calculated and scaled vibrational wave numbers and the detailed description of each normal mode of vibration of MPOA carried out in terms of their contribution to the total potential energy are given in Table 2.

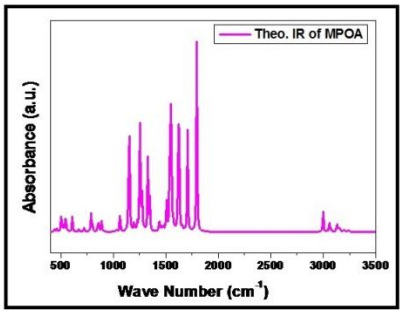

Figure 4. Theoretical IR Spectra of MPOA.

Table 2. Vibrational analysis of prominent modes of MPOA at B3LYP/6-311++G(d,p) level.

Cal. Frequency ($incm^1$)	Scaled Frequency (in cm^{-1})	IR Intensity (cal.) (a.u.)	Assignment
3621	3493	22.6	υ[(N2-H29)(100)]
3604	3477	45.3	υ(N6-H30)(100)
3242	3128	7.6	υ(C15-H16)(98)
3206	3093	10.1	υ(C10-H11)(98)
3189	3077	4.7	υ (C13-H14)(98)
3158	3047	8.2	υ (C18-H19)(100)
3147	3036	16.6	υ(C7-H8)(97)
3132	3022	25.7	υ (C25-H26)(92)
3121	3011	0.0311	υ_{as} [(C21-H22)(50)+ (C21-H23)(50)]
3074	2966	9.5	υ_{s}[(C21-H22)(50)+C(21-H23)(50)
3056	2948	41.4	υ_{as}[(C25-H27)(50)+(C25-H28)(50)]
3000	2894	76.3	υ_{s}[(C25-H27)(46)+(C25-H28)(-46)]
1795	1732	689.4	υ[(O9-C24)(84)]
1707	1647	350.0	υ_{as}[(O5-C17)(58)+C20-C18)(14)]
1657	1599	12.8	υ[(C15-C13)(29)]
1627	1570	320.0	υ(C12-C10)(25)
1619	1562	352.4	υ_{s}[(O5-C17)(16)+(C20-C18)(43)]
1552	1497	559.9	β[(H29-N2-C4)(40)]
1539	1485	358.8	β[(H8-C7-H10)(17)]
1506	1453	100.7	β[(H28-C25-H27)(54)]
1492	1439	9.0	β[(H26-C25-H28)(38)+ (H27-C25-H26) (38)]+τ_i [(H26-C25-O3-C12)(16)]
1475	1422	21.0	β[(H26-C25-H28)(30)+(H27-C25-H26)(30)+(H28-C25-H27)(23])
1461	1411	6.1	β[(H30-N6-C24)(18)+(H23-C21-H22)(27)]
1454	1403	15.7	β[(H23-C21-H22)(58
1438	1387	52.1	υ[(C15-C13)(21)]
1347	1300	115.7	β(H30-N6-C24)(17)
1333	1286	35.4	β[(H8-C7-C10)(17)]
1327	1280	240.1	υ[(C4-C7)(13)]
1291	1246	6.8	υ[(O3-C12)(22)]
1255	1211	290.7	τ_i[(H22-C21-S1-C20)(16)+(H23-C21-S1-C20)(18)]
1250	1206	163.3	υ[(N2-C4)(18)]
1227	1184	31.4	τ_i[(H22-C21-S1-C20)(-15)+(H23-C21-S1-C20)(18)]
1202	1160	13.7	β[(H28-C25-H27)(16)+τ_i[(H27-C25-O3-C12)(30)+(H28-C25-O3-C12)(30)]
1198	1156	20.4	β[(H8-C7-C10)(23)] +(H11-C10-C7)(22)]
1168	1127	0.7	τ_i[(H26-C25-O3-C12)(35)+(H27-C25-O3-C12)(18)+(H28-C25-O3-C12)(18)]
1151	1110	510.2	υ[(N2-C17)(24),(N6-C20)(15)]+β[(H19-C18-C20)(20)]
1142	1109	0.0431	β[(H22-C21-S1)(49)]+τ_i[(H23-C21-S1-C20)(27)]
1139	1099	52.8	β[(H14-C13-C15)(21)+(H16-C15-C13)(21)]
1063	1026	74.2	υ[(O3-C25)(72)]
1031	995	5.2	υ[(C18-C17)(27)]
1022	986	0.1	β[(C15-C13-C12)(37)+(C12-C10-C7)(22)]
987	952	0.7	τ_i[(H14-C13-C15-C4)(23)+ (H16-C15-C4-N2()59)]
915	883	0.4	τ_i[(H8-C7-C4-N2)(41)+ (H11-C10-C7-C4)(22)+(C4-C7-C10-C12)(24)]
908	876	3.4	β[(H22-C21-S1)(48)]+τ_i[(H22-C21-S1-C20)(18)]
890	859	41.0	υ[(N6-C24)(18) +(C21-C24)(52)]
866	836	2.5	β[(C13-C12-C10)(25)]
856	826	47.6	τ_i[(H14-C13-C15-C4)(47)+ (H16-C15-C4-N2)(28)]
802	774	2.1	β[(O5-C17-C18)(25)]
802	774	21.6	τ_i[(H8-C7-C4-N2)(43)+(H11-C10-C7-C4)(45)]
787	759	51.0	τ_i[(H19-C18-C20-N6)(56)+[(O5-N2-C18-C17)(37)]
787	759	12.2	β[(C21-C24-N6)(20)]
762	735	0.6	β[(C21-C24-N6)(42)]
729	703	4.7	τ_o(N2-C15-C7-C4)(16)
722	697	13.8	τ_i[(H19-C18-C20-N6)(27)+τ_o[(O5-N2-C18-C17)(38)]
700	675	8.0	β[(S1-C20)(63)]
666	643	4.1	β[(C24-N6-C20)(24)]
645	622	0.4	β[(C4-C7-C10)(17),+(C15-C13-C12)(17),+(C12-C10-C7)(24)]
609	588	53.6	τ_i[(N30-N6-C24-C21)(40)+τ_o[(O9-C21-N6-C24)(40)]
552	533	24.1	τ_o[(S1-N6-C18-C20)(69)]
546	527	50.7	β[(C25-O3-C12)(23)]
529	510	14.0	τ_o[(O3-C10-C13-C12)(28)+(N2-C15-C7-C4)(32)]
519	500	9.2	τ_i[(H30-N6-C24-C21)(41)+τ_o[(O9-C21-N6-C24)(24)]
509	491	23.6	β[(O9-C24-N6)(-21)+(N6-C20-C18)(23)]
501	483	46.8	τ_i[(H29-N2-C4-C15)(68)]
463	447	10.2	β[(S1-C20-C18)(15)+(O9-C24-N6)(22)+ (C24-N6-C20)(23)]
441	425	8.4	β[(S1-C20-C18)(17)+(O3-C12-C13)(18)]
422	407	0.3	τ_i[(C15-C13-C12-C10)(33)+ (C13-C12-C10-C7)(24)]
381	368	1.2	τ_i[(C4-C7-C10-C12)(24)+τ_o[(O3-C10-C13-C12)(24)+(N2-C15-C7-C4)(15)]
364	351	1.0	β[(N2-C4-C7)(28)]
311	300	13.4	β[(O5-C17-C18)(19)+(N6-C20-C18)(20)]
252	243	0.8	τ_i[(H26-C25-O3-C12)(26)]

Cal. Frequency (incm^1)	Scaled Frequency (in cm^{-1})	IR Intensity (cal.) (a.u.)	Assignment
247	238	8.0	β[(O3-C12-C13)(30)+ (C18-C17-N2)(15)+ (C25-O3-C12)(24)]
228	220	0.2	τ_i[(N6-C20-C18-C17)(32)]
163	157	0.6	τ_i[(C13-C12-C10-C7)(28)]
151	146	5.0	β[(C20-C18-C17)(18)+(N2-C4-C7)(29)]
139	134	0.0089	τ_i[(C20-C18-C17-N2)(19)+ (C24-N6-C20-C18)(19)+(C21-C24-N6-C20)(16)]
91	88	0.0035	τ_i[(C24-N6-C20-C18)(15)+(C25-O3-C12-C10)(39)]
85	82	18.3	τ_i[C21-C24-N6-C20)(35)]
63	61	0.0497	τ_i[(C20-C18-C17-N2)(26)+(C25-O3-C12-C10)(26)]
52	60	0.3	β[(C20-C18-C17)(29)+ (C17-N2-C4)(23)+(C18-C17-N2)(28)]
35	34	0.1	τ_i[(C17-N2-C4-C15)(36)+ (N6-C20-C18-C17)(16)+ (C18-C17-N2-C4)(29)]
21	20	0.2	τ_i[(C20-C18-C17-N2(25)+ (C17-N2-C4-C15)(34)+ (C18-C17-N2-C4)(20)]

Where υ, υ_s, υ_{as} is stretching, symmetry stretching and antisymmetry stretching β is bending andτ_i, τ_o is in plane ,out plane torsion respectively.

C-H Vibrations inBenzene and Five member ring. Generally the aromatic C-H stretching modes are found in the region 3100–3000cm $^{-1}$. For the title compound the C-H stretching vibration found in the range 3128 -3011 cm^{-1}[15,16] Also in five member ring the C-H asymmetry stretching vibration occurred in the region 2948 cm^{-1}. The calculated values are good agreement with standard value.

*C-C Vibrations.*The C-C ring stretching vibrations are expected within the region 1650-1200 cm^{-1}. Most of these ring modes are altered by the substitution to aromatic ring. The Calculated frequencies for C−C and C=C stretching modes at B3LYP/6-311++*G(d,p)* are 1599 -1618 cm^{-1}, 1562 cm^{-1} and in five member ring 995- 859 cm^{-1}. Some other C−C modes associated with bending, torsion vibrations of ring are also found in lower frequency region as well as overlapping with other modes, also C-C-C- and C-C-C-C modes have a frequency in the rang 986 -157 cm^{-1}. Most of C−C modes are comparatively stronger than C−H modes.

*N-H Vibrations.*The N–H stretching vibrations are normally viewed in the region 3300–3600 cm^{-1}. For title compound the N–H stretching vibration presented at 3493-3477 cm^{-1} this is a pure stretching mode which is evident from its contribution of 100% to the total Potential Energy Distribution (P.E.D).All theoretical wavenumbers due to N–H stretching calculated by B3LYP/6-311++G(d,p) method are in good agreement with the results of GurkanKesan and coworkers [17].

C=O Vibrations. The frequency of a vibration is directly related to the strength of the bond i.e. force constant hence C=O stretching will be higher than C-C and C-O stretching respectively. The standard vibrational frequency of C-O follows in region 1700-1200 cm^1.The calculated C-O scaled vibrational frequency by B3LYP/6-311G ++(d,p) normally follows lies in the range 1731-1026 cm^{-1} which is a nearly good agreement with standard values[18].

*C-S Vibrations.*The C-S stretching follows in the range 710-570 cm^{-1}. For the title compound the C-S stretching bond occurs in the range 670 cm^{-1} which is in good agreement.

3.5. Global and local reactivity descriptors.

The global chemical reactivity descriptors such as electron affinity, ionization potential, chemical potential, electronegativity, hardness, softness and electrophilicity index and local reactivity descriptor likeFukui functions have also been calculated using DFT. The electronic chemical potential can be calculated as μ = -(IP + EA)/2 which describe the escaping propensity of the electron from a stable system. The negative value of the electronic chemical potential is defined as Electronegativity (χ). Chemical hardness correlated with the stability and reactivity of the chemical system, which shows the resistance to alteration in electron distribution is given by η = (IP– EA)/2. The global softness S = (1/η) is inverse of the hardness [19]. Further the global electrophilicity index (ω), introduced by Parr et al. [20] is calculated in terms of chemical potential and the hardness by the relation $\omega = \mu^2/2\eta$ and give the lowering of energy due to maximal electron flow between donor and acceptor. Here the ionization potential (IP) and electron affinity (EA) are defined as the difference in the ground state energy between the cationic and neutral system and difference in the ground state energy between neutral and anionic system i.e. IP = E(N -1) - E(N) and EA = E(N) -E(N + 1). The calculated values of these global reactivity descriptors for the title molecule were collected in Table3. The value of chemical hardness is 2.07 eV. Considering the chemical hardness, if one molecule has a large HOMO–LUMO gap, it is a hard molecule or small HOMO–LUMO gap it is a soft molecule. One can also relate the stability of molecule to hardness, which means that the molecule with least HOMO–LUMO gap means it is more reactive[20]. The local reactivity descriptor like Fukui function indicates the preferred regions where a chemical species (molecule) will amend its density when the number of electrons ismodified or it indicates the tendency of the electronic density to deform at a given position upon accepting or donating electrons [21,22].

Table 3. Electronic parameters of MPOA calculated at B3LYP/6-311++ G(d,p) level.

Parameters	Formula	Values
Ionization potential (eV)	IP= -E_{HOMO}	5.69 eV
Electron affinity (eV)	EA= -E_{LUMO}	1.55 eV
Electronic chemical potential	μ= -(IP+EA)/2	-3.62eV
Absolute electronegativity(eV)	χ =(IP+EA)/2	3.62 eV
Chemical hardness (eV)	η = (IP-EA)/2	2.07 eV
Chemical softness(eV)	S= 1/η	0.48 eV
Electrophilic index (eV)	ω = χ^2 /2η	3.17 eV

The condensed or atomic Fukui functions on the kth atom site, for electrophilic (f_k^-), nucleophilic (f_k^+) and free radical (f_k^0) attacks are defined as f_k^+ = [q(N+1) - q(N)] , f_k^-=[q(N) - q(N-1)andf_k^0 = 1/2[(q(N+1) - q(N-1)] respectively, where q_k is the atomic charge (NBO) at the kth atomic site in the anionic (N + 1), cationic (N -1) or neutral molecule. Parr and Yang [19,20]showed

that sites in chemical species with the largest values of Fukui function (f_k) show high reactivity for corresponding attacks. The Fukui functions calculated from the NBO charges have been reported to be in good acceptation [23,24].

Table 4. Values of the condensed Fukui functions of MPOA considering NBO charges.

Atoms	f_k^+	f_k^-	f_k^0
S1	0.10496	0.09106	0.09801
N2	0.09105	0.01868	0.054865
O3	0.09316	0.01734	0.05525
C4	0.07081	0.00075	0.03578
O5	**0.84579**	0.08251	**0.46415**
N6	0.01548	-0.01123	0.002125
C7	-0.3893	0.05268	-0.16831
H8	0.02729	0.01228	0.019785
O9	0.0536	0.10961	0.081605
C10	0.03835	0.00684	0.022595
H11	0.02742	0.01805	0.022735
C12	0.0822	0.05827	0.070235
C13	0.03948	0.02653	0.033005
H14	0.02867	0.01706	0.022865
C15	0.03029	0.00921	0.01975
H16	0.02097	-0.00182	0.009575
C17	-0.01844	0.0753	0.02843
C18	0.04765	0.0672	0.057425
H19	0.0151	0.02462	0.01986
C20	0.02013	**0.11403**	0.06708
C21	-0.00295	-0.0126	-0.00777
H22	0.02233	0.0422	0.032265
H23	0.02233	0.04221	0.03227
C24	-0.00125	0.07956	0.039155
C25	-0.01706	-0.00524	-0.01115
H26	0.0267	0.01553	0.021115
H27	0.02146	0.00863	0.015045
H28	0.02147	0.00862	0.015045
H29	0.02171	0.01239	0.01705
H30	0.01246	0.01973	0.016095

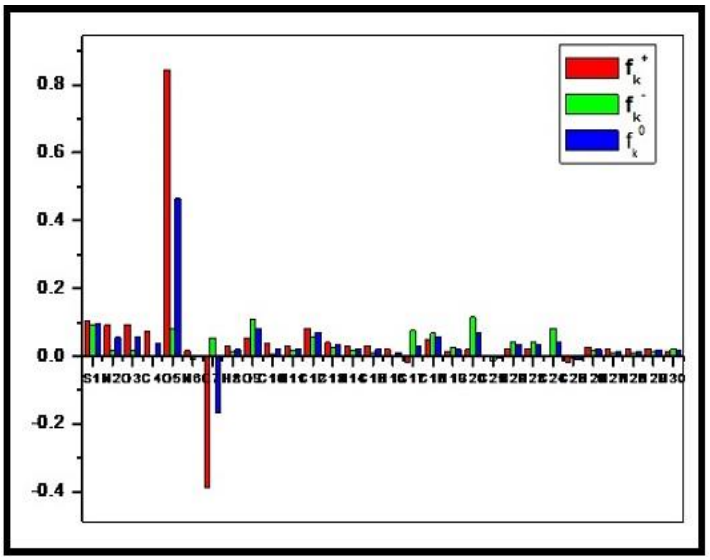

Figure 5. Fukui functions considering NBO charges of MPOA.

In the present case values of calculated Fukui functions based on NBO charges, given in Table 4, indicates that in MPOAcompound the reactivity order for the nucleophilic case is O5 > S1 > O3> N2 > C12 > C14 >O9 >C18 and the electrophilic reactivity order is C20 > O9 > S1 > O5 >C24 >C17 >.C18 >C12 while the order of sites for free radicals attack is O5 > S1 > O9 >C12 >C20 >C18 >O3 >N2. Also the graphical representation fukui function of MPOA is shown in fig.5

4. CONCLUSIONS

The present study reveals that MPOA may be a significant agent for biological and pharmacological applications. The optimized geometric parameters of the compound are in good agreement that of its experimentallydetermined values.MESP surface and various electronic parameters have been calculated in order to analyze the chemical reactivity of MPOA.A comprehensive vibrational analysis along with normal mode assignment has been done for the compound to complement the IR spectra.The calculated Fukui functions value indicate that susceptible sites forelectrophilic addition are in order of C20 > O9 >S1 > O5 >C24 >C17 >.C18 >C12 while O5 > S1 > O3> N2 > C12 > C14 >O9 >C18 are the order of sites prone to nucleophilic attack. The present study of MPOA, in general, may lead to the better understanding of the compound in terms of electronic properties and its vibrational modes and may help in designing and synthesizing new efficient materialsfor biological and pharmacological application.

5. REFERENCES

1. Trotsko, N.; Kosikowska, U.; Paneth, A.; Plech, T.; Malm, A.; a Wujec, M. Synthesis and Antibacterial Activity of New Thiazolidine-2,4-dione-Based Chlorophenylthiosemicarbazone Hybrids. *Molecules***.** **2018**, *23*, 1023, https://doi.org/10.3390/molecules23051023.

2. Rajareddy, A.; Murthy, M.S. Design, synthesis and characterization of novel benzothiazole derivatives containing thiazolidine-2, 4-dione for anti-cancer screening. *The Pharma Innovation Journal* **2019**, *8*, 175-180.

3. Upadhyay, M.; Asif, M.; Sahu, K.; Asati, V.; Rathi, J. C. 2d- and 3d-qsar studies on thiazolidine-2,4-dione derivatives. *World journal of pharmacy and pharmaceutical sciences* **2019,** 8, 662-678.

4. Bataille, C.J.R.; Brennan, M.B.; Byrne, S.; Davies, S.G.; Durbin, M.; Fedorov, O.; Huber,K.V.M., Jones, A.M.; Knapp, S.; Liu, G.; Nadali, A.; Quevedo, C.E.; Russell, A.J.; Walker, R.G.; Westwood, R.; Wynne, G.M. Thiazolidine derivatives as potent and selective inhibitors of the PIM kinase family. *Bioorganic &Medicinal Chemistry* **2017**, *25*,2657-2665, https://doi.org/10.1016/j.bmc.2017.02.056.

5. Upadhyay, A.; Srivastava, S.K.; Srivastava, S.D. Conventional and microwave assisted synthesis of some new N-[(4-oxo-2-substituted aryl-1,3-thiazolidine)acetamide]-5-nitroindazoles. *Eur. J. Med. Chem*. **2010**, *45*, 3541–3548, http://dx.doi.org/10.1016/j.ejmech.2010.04.029.

6. Sayyed, M.; Mokle, S.; Bokhare, M.; Mankar, A.; Surwase, S., Bhusare, S., Vibhute, Y. Synthesis of some new 2,3-diaryl-1,3-thiazolidin-4-ones as antibacterial agents. *Arkivoc* **2006**, *2***,** 187–192.

7. Visagaperumal, D.; Kumar, R.J.; Vijayaraj, R.; Anbalagan, N. Microwave-induced synthesis of some new 3-substituted-1, 3-thiazolidin-4-ones for their potent antimicrobial and antitubercular activities. *Int. J. Chem. Tech. Res*. **2009**, *4*, 1048–1051.

8. Kato, T.; Ozaki, T.; Tamura, K.; Suzuki, Y.; Akima, M.; Ohi, N. Novel calcium antagonists with both calcium overload inhibition and antioxidant activity.2. Structure-activity relationship of Thiazolidinone derivatives. *J. Med. Chem.* **1999**, *42*, 3134-3146, https://doi.org/10.1021/jm9900927.
9. Apostolidis, I.; Liaras, K.; Geronikaki, A.; Hadjipavlou - Litina, D.; Gavalas, A.; Sokovic,M. Synthesis and biological evaluation of some 5-arylidene-2-(1,3-thiazol-2-ylimino)-1,3-thiazolidin-4-ones as dulal anti-inflammatory/antimicrobial agents. *Bioorg. Med. Chem.* **2013**, *21*, 532-539, https://doi.org/10.1016/j.bmc.2012.10.046
10. Makwana, H.R.; Malani, A.H. A Brief Review Article: Thiazolidines Derivatives and Their Pharmacological Activities. *Journal of Applied Chemistry* **2017,** *10*, 76-84,
11. Becke, A.D. Density-functional thermochemistry.III. The role of exact exchange. *J. Chem. Phys*. **1993**, *98*, 5648–5652, https://doi.org/10.1063/1.464913.
12. Lee, C.; Yang, W.T.; Parr, R.G. Development of the colle-salvetti correlation-energy formula into a functional of electron density. *Phys. Rev*. **1988**, *37*, 785–789, https://doi.org/10.1103/physrevb.37.785.
13. Merrick, J.P.; Moran, D.; Radom, L. An evaluation of harmonic vibrational frequency scale factors. *J. Phys. Chem. A* **2007**, *111*, 11683–11700, https://doi.org/10.1021/jp073974n.
14. Galushchinskiy, A.; Slepukhin, P.; Obydennova. K. Crystal structures of two (Z)-2-(4-oxo-1, 3-thiazolidin-2-ylidene)acetamides. *ActaCryst*. **2017**, *73*, 1850–1854, https://dx.doi.org/10.1107%2FS2056989017016061.
15. George, J.; Prasana, J.C.; Muthu, S.; Kuruvilla, T.K. Spectroscopic (FT-IR, FT Raman) and Quantum Mechanical Study on Isosorbide Mononitrate by Density Functional Theory. *International Journal of Materials Science* **2017,** *12*, 302-320.
16. Solaichamy, R.; Karpagam, J. Molecular Structure, Vibrational Spectra and Docking Studies of Abacavir by Density Functional Theory. *International Letters of Chemistry, Physics and Astronomy* **2017**, *72*, 9-27, https://doi.org/10.18052/www.scipress.com/ILCPA.72.9.
17. Baglayan, O.;Kesan, G.; Parlak, C.; Alver, O.; Enyel, M.S. Vibrational investigation of 1-cyclopentylpiperazine. *Sci. China Phys. Mech. Astron* **2014**, *57*, 1654–1661, http://dx.doi.org/10.1007/s11433-013-5313-0.
18. Yadav, K.K.; Kumar, A.; Kumar, A.; Misra, N.; Brahmachari, G. Structure, spectroscopic analyses (FT-IR and NMR), vibrational study,chemical reactivity and molecular docking study on 3,3'-((4-(trifluoromethyl)phenyl)methylene)bis(2-hydroxynaphthalene-1,4-dione), a promising anticancerousbis-lawsone derivative. *Journal of Molecular Structure* **2018,** *1153*, 1-10, https://doi.org/10.1016/j.molstruc.2017.09.095.
19. Parr, R.G.; Pearson,R.G. Absolute hardness: companion parameter to absolute electronegativity.*J. Am. Chem. Soc.* **1983**, *105*, 7512–7516, https://doi.org/10.1021/ja00364a005.
20. Abbaz, T.; Bendjeddou, A.; Villemin, D. Molecular structure, HOMO, LUMO, MEP, natural bond orbital analysis of benzo and anthraquinodimethane derivatives. *Pharmaceutical and Biological Evaluations* **2018**, *5*, 27-39, http://dx.doi.org/10.26510/2394-0859.pbe.2018.04.
21. Parr, R.G.; Yang, W. *Functional Theory of Atoms and Molecules.* Isted.; Oxford University Press:New York, U.S.A., 1989
22. Parr, R.G.; Yang,W. Density functional approach to the frontier- electron theory of chemical reactivity. *J. Am. Chem. Soc*. **1984**, *106*, 4048–4049
23. Nazari, F.; Zali, F.R. Density functional study of the relative reactivity of carbonyl group in substituted cyclohexane.*J. Mol. Struct. (Theochem)* **2007**, *817*, 11–18, https://doi.org/10.1021/ja00326a036.
24. Macias, M.Á.Z.; Chavez, M.M.G.; Mendez, F.; Chavez, R.G; Richaud, A. Theoretical Reactivity Study of Indol-4-Ones and Their Correlation with Antifungal Activity. *Molecules* **2017**, 22, 427, https://doi.org/10.3390/molecules22030427.

6. ACKNOWLEDGEMENTS

Prem Chandra Maurya gratefully acknowledges Council of Scientific and Industrial Research (CSIR), New Delhi, India for a research fellowship [Grant No. 09/107(0401)/2018-EMR-I] and Central Facility for Computational Research (CFCR) University of Lucknow for providing computational time.